Science in China Series D: Earth Sciences

www.scichina.com
earth.scichina.com
www.springerlink.com

Links between global CO_2 variability and climate anomalies of biomes

ZHOU Tao[1,2†], YI ChuiXiang[3], Peter S. BAKWIN[4] & ZHU Li[5]

[1] State Key Laboratory of Earth Surface Processes and Resource Ecology, Beijing Normal University, Beijing 100875, China;
[2] College of Resources Science and Technology, Beijing Normal University, Beijing 100875, China;
[3] School of Earth and Environmental Sciences, Queens College, City University of New York, New York 11367, USA;
[4] NOAA Climate Monitoring and Diagnostics Laboratory, 325 Broadway, Boulder, CO 80305, USA;
[5] Department of Epidemiology and Biostatistics, Texas A & M University, College Station, TX 77843, USA

The global rate of fossil fuel combustion continues to rise, but the amount of CO_2 accumulating in the atmosphere has not increased accordingly. The causes for this discrepancy are widely debated. Particularly, the location and drivers for the interannual variability of atmospheric CO_2 are highly uncertain. Here we examine links between global atmospheric CO_2 growth rate (CGR) and the climate anomalies of biomes based on (1986—1995) global climate data of ten years and accompanying satellite data sets. Our results show that four biomes, the tropical rainforest, tropical savanna, C_4 grassland and boreal forest, and their responses to climate anomalies, are the major climate-sensitive CO_2 sinks/sources that control the CGR. The nature and magnitude by which these biomes respond to climate anomalies are generally not the same. However, one common influence did emerge from our analysis; the extremely high CGR observed for the one extreme El Niño year was caused by the response of the tropical biomes (rainforest, savanna and C_4 grassland) to temperature.

biomes, carbon cycle, climate anomaly, NDVI, El Niño

Rising atmospheric CO_2 concentration, due to fossil fuel combustion and deforestation, has resulted in global warming[1]. Recent analyses of the global carbon cycle indicate that terrestrial ecosystems sequester a significant proportion of anthropogenic CO_2, and less than half of the annual anthropogenic emissions of CO_2 remain in the atmosphere[2]. However, the rate of CO_2 accumulation in the atmosphere over the past "has remained the same or even declined slightly" in spite of the fact that fossil fuel emissions have increased by almost 40% over the same time period[3]. The cause of year-to-year variations in atmospheric CO_2 accumulation is highly uncertain[3−6].

The atmospheric CO_2 concentration is mainly controlled by anthropogenetic emissions, ocean-atmosphere flux, and land-atmosphere flux. Despite annual anthropogenetic emissions increased steadily, the observed atmospheric CO_2 growth rate (CGR) did not show a similar increasing trend but presented apparently interannual variations[5]. Therefore, the CGR presents the net effect of several processes that regulate global land-atmosphere and ocean-atmosphere fluxes, whose year-to-year fluctuations are associated with major climatic events[7].

Two conventional methods have been used to partition this variability between the ocean and land. The top-down (inverse) method[8] is based on atmospheric measurements of CO_2, O_2 and $^{13}CO_2$, as high-precision atmospheric observations of concentrations of CO_2 and O_2 (as O_2:N_2 ratio) make it possible to partition the uptake of atmospheric CO_2 between the land and ocean[9].

Received August 30, 2007; accepted December 24, 2007
doi: 10.1007/s11430-008-0024-5
†Corresponding author (email: tzhou@bnu.edu.cn)
Supported by the National Natural Science Foundation of China (Grant Nos. 40401028, 40671173, 40425008, and 30590384) and the Visiting-Professor Funding from the Institute of Geographical Sciences and Natural Resources (IGSNRR), Chinese Academy of Sciences

The bottom-up method[10], however, is based on inventories of land-use change and forest coverage.

Studies indicate that the variability of fossil fuel emissions and the estimated variability in net ocean uptake are too small to account for the variations of CGR, which must be caused by year-to-year fluctuations in land-atmosphere fluxes[7]. Both ocean models and ocean observations robustly attribute little variability to ocean-atmosphere CO_2 flux, with the value of ± 0.5 GtC$\cdot$a^{-1} between extremes[11−13]. Contrarily, the interannual variability of global land-atmosphere fluxes is much larger than that of air-sea fluxes, with the value of ± 4 GtC$\cdot$a^{-1} between extremes[14−16].

A predominantly terrestrial origin of the growth rate variability can be inferred from different researches, including (1) atmospheric inversions assimilating time series of CO_2 concentrations from different stations[14−16], (2) consistent relationships between $\delta^{13}C$ and CO_2[9], (3) ocean model simulations[12,13], and (4) terrestrial carbon cycle and coupled model simulations[17−20].

Although both top-down and bottom-up methods have identified that the interannual variations of CGR are controlled by the land-atmosphere fluxes associated with major climatic events, there still have many uncertainties on regional fluxes. For the top-down methods, the errors are usually higher for individual regions (continents or ocean basins) and the significance can be lost. For the bottom-up methods, however, the observations of land ecosystem carbon fluxes are too sparse and the ecosystems are too heterogeneous to allow global assessment of the net land flux with sufficient accuracy[7].

Under the background that the interannual variability in the growth rate of atmospheric CO_2 is dominated by the response of the land biosphere to climate variation[7], the year-to-year variations in the global atmospheric CO_2 growth rate are mainly caused by natural processes, so links between the CGR and the key climate factors that control the terrestrial carbon cycle should exist.

In this study, we analyzed the relationship between global atmospheric CO_2 growth rate and climate variables on biome scale. The analysis is done on a simple premise that world biomes are controlled by climate primarily through influences on the ability of the biome to exchange CO_2 and H_2O with the atmosphere. We assume current equilibrium between biome distribution and the existence of a compatible climate, such that climate characteristics at the centroid probability for biome distribution reflect the optimum (Figure 1).

1 Materials and methods

We took the average of the 48 quasi-weeks growth rates in each year from the GLOBALVIEW-CO_2 database in NOAA/CMDL as the annual mean growth rate in CO_2 concentration[21]. The land cover data set[22] used was based on advanced very high resolution radiometer's (AVHRR) maximum monthly composites for Normalization Difference Vegetation Index (NDVI) values in 1987 at approximately 8 km resolution, averaged to 1°×1° resolution. This NDVI-derived land cover classification was also combined with three existing ground-based data sets[23−25] of global land cover.

Annual mean air temperatures were obtained from the Global Historical Climatology Network (GHCN version 2) that contains approximately 1260 to 5860 terrestrial stations available for monthly air temperature records[26] for the period from 1950 through 1999. We merged the temperature data sets from 0.5°×0.5° to 1°×1° resolution to keep the same spatial resolution as the land cover. We acquired annual precipitation data from the datasets of grid monthly area-mean precipitation for the global land surface and the period from January 1986 to March 1999 on a 1°×1° grid. These datasets were produced by the Global Precipitation Climatology Center (GPCC) based on rain gauge observations worldwide from about 7000 meteorological stations[27]. GPCC collects monthly precipitation totals received from CLIMAT and SYNOP reports via the World Weather Watch GTS (Global Telecommunication System) of the World Meteorological Organization.

Annual photosynthetically active radiation (PAR) and net radiation (R_n) were calculated from the monthly global datasets of surface shortwave (SW) and long wave (LW) fluxes with 1°×1° resolution[28]. These SW and LW fluxes were produced by the NASA/Global Energy and Water Cycle Experiment (NASA/GEWEX) Surface Radiation Budget (SRB) project with one detailed radiative transfer model and one parameterized model (quality-check SW and LW models). These models are driven with a number of input datasets, such as cloud properties derived from the International Satellite Cloud Climatology Project (ISCCP) DX data, and meteorological profiles obtained from the Goddard GEOS-1 data assimilation product. Both SW models used clear-sky albedo at the top of atmosphere from the

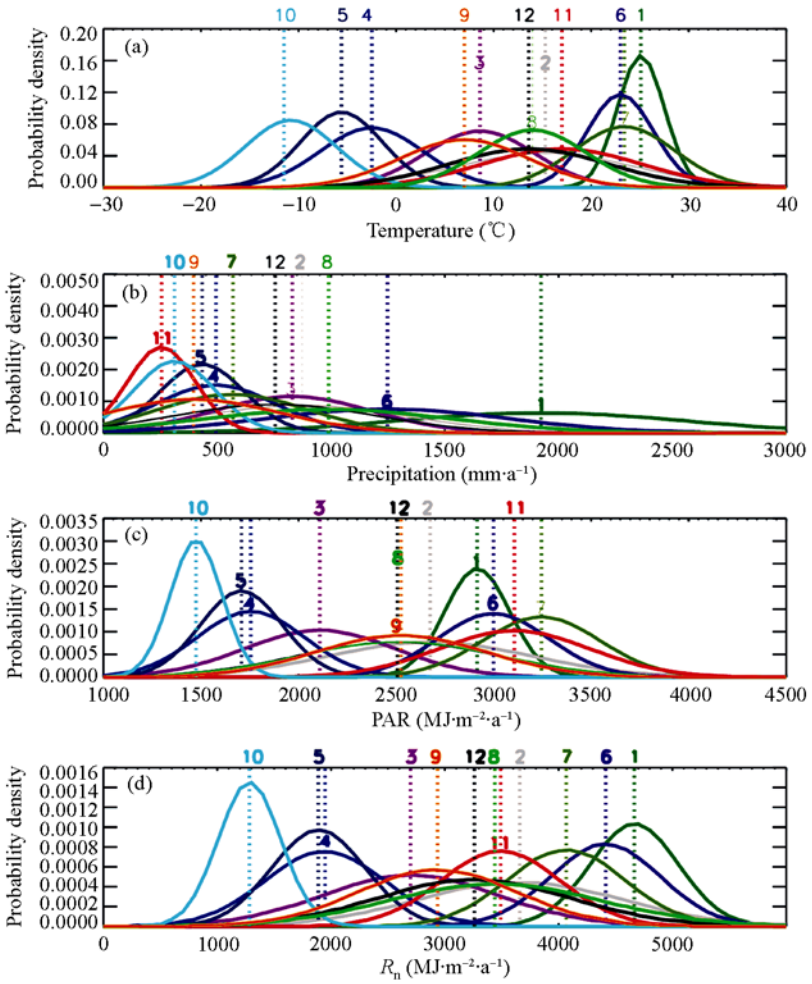

Figure 1 Climatic envelopes of biomes. (a) Temperature; (b) precipitation; (c) photosynthetically active radiation (PAR); and (d) net radiation. The numbers centered above each curve are biome codes listed in Table 1. These curves were obtained based on 10-year globally climatic data sets with 1°×1° resolution.

Earth Radiation Budget Experiment (ERBE).

Our analysis focuses on the period of 1986—1995 when data for all climate factors were available, except for PAR and R_n data for November and December of 1995. We used nine-year monthly mean values to fill these two months for the missing data for each grid cell. We calculated globally ten-year averages and standard deviations of climate variables (T, P, PAR, and R_n) for each biome defined by the NDVI-derived land cover data sets. We also calculated the global annual mean value of each climate variable for each biome. The difference between the one-year and 10-year averages of each climate variable for each biome is defined as a "climate anomaly". We derived Budyko's dryness index for the biome scale based on net radiation and precipitation data. Dryness index was defined as Dryness=$R_n/(L\times P)$, where R_n (MJ·m^{-2}·a^{-1}) and P (mm·a^{-1}) are global annual mean net radiation and precipitation for a biome respectively, and L=2.5 MJ·kg^{-1} is the enthalpy of vaporization. We excluded a method to calculate the dryness index on a grid cell because annual precipitation for some grid cells was so low that it would make the dryness index infinite.

2 Results and discussions

All significant correlations between the CGR and climate anomalies of biomes listed in Table 1 are shown in Figure 2. The CGR is positively correlated to precipitation anomalies and negatively to dryness anomalies for the tropical rain forest biome (Figure 2(a) and (b)). One obvious outlier in the data set is seen in 1987 (Figure 2(a) and (b)). The correlations between the CGR and precipitation or dryness anomalies are much improved if

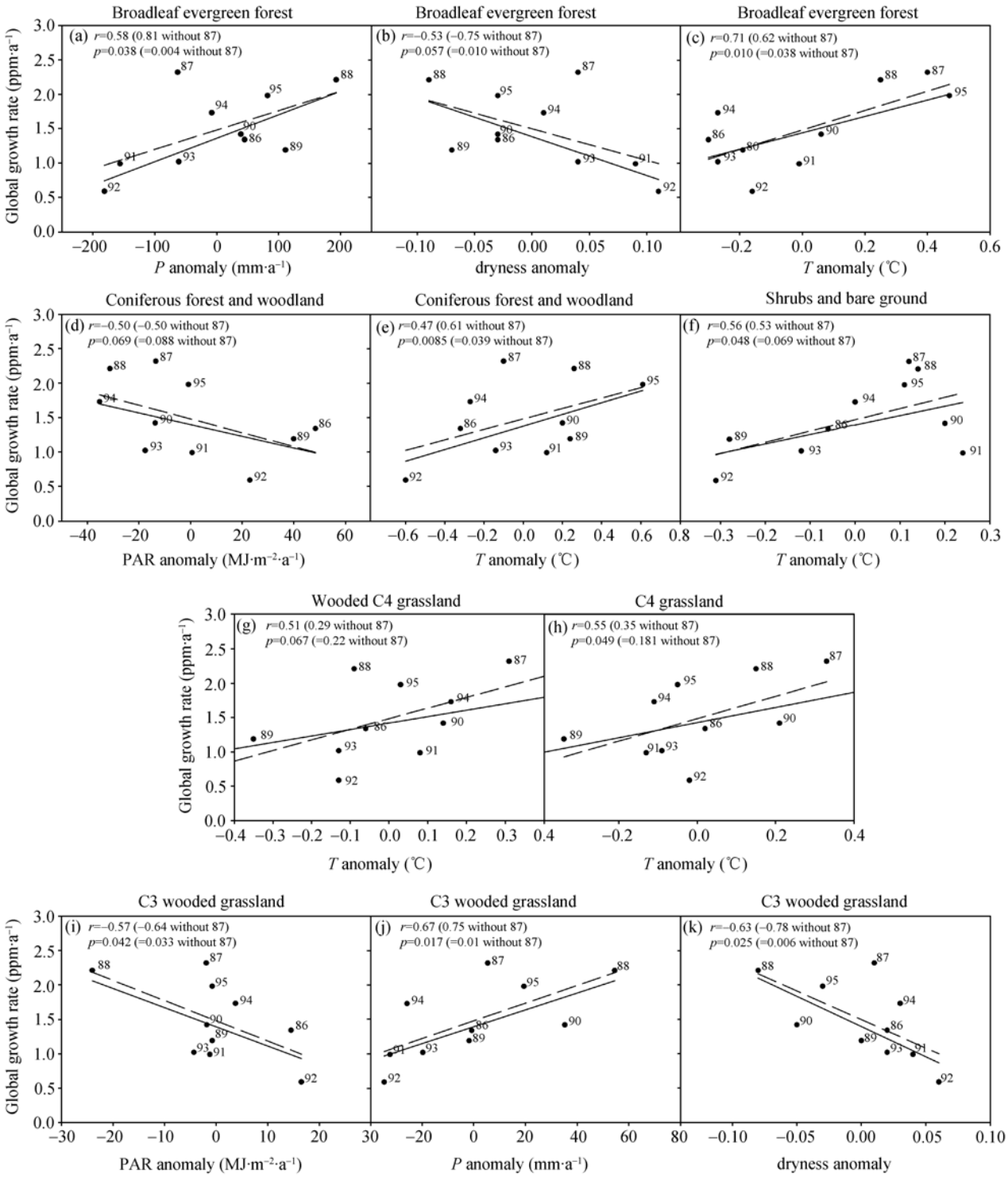

Figure 2 Significant correlation between the global atmospheric CO_2 growth rates and the anomalies of each climate factor for each biome. Numbers on the data points indicate years. The solid line is a linear regression excluding 1987 and the dash line is a linear regression including 1987.

data for 1987 are excluded. We note that 1987 was an El Niño year. The CGR is highly correlated to temperature anomalies of the tropical rain forest biome (Figure 2(c)). This observation is supported by past site-specific field studies that have demonstrated reduced photosynthesis and enhanced respiration in tropical forest ecosystems during the years of the warmest temperature[29,30].

The CGR was negatively correlated with PAR anoma-

Table 1 Climate characteristics of biomes (ten-year average, 1986—1995). The numbers in parentheses are standard deviations

Code	Biome	P ($mm \cdot a^{-1}$)	T (℃)	PAR ($MJ \cdot m^{-2} \cdot a^{-1}$)	R_n ($MJ \cdot m^{-2} \cdot a^{-1}$)	Dryness	Area (10^6 km^2)
1	Broadleaf evergreen forest	1922 (629)	25.1 (2.4)	2916 (167)	4664 (387)	0.97 (0.07)	13.4
2	Broadleaf deciduous forest and woodland	872 (458)	15.3 (9.2)	2675 (517)	3658 (902)	1.68 (0.05)	3.3
3	Mixed coniferous and broad-leaf deciduous forest and woodland	830 (347)	8.6 (5.6)	2109 (387)	2698 (774)	1.30 (0.06)	6.6
4	Coniferous forest and wood-land	494 (265)	-2.5 (5.3)	1755 (276)	1948 (529)	1.58 (0.07)	13.0
5	High latitude deciduous forest and woodland	434 (184)	-5.6 (4.2)	1707 (210)	1889 (411)	1.74 (0.09)	5.8
6	Wooded C4 grassland	1248 (528)	23.0 (3.4)	2999 (285)	4413 (482)	1.42 (0.06)	17.1
7	C4 grassland	569 (328)	23.4 (5.2)	3245 (301)	4066 (518)	2.87 (0.16)	8.9
8	C3 wooded grassland	990 (538)	14.0 (2.4)	2523 (515)	3440 (933)	1.39 (0.04)	4.6
9	C3 grassland	396 (378)	7.0 (2.4)	2525 (435)	2936 (705)	2.97 (0.18)	11.5
10	Tundra	312 (176)	–10.8 (4.7)	1475 (132)	1283 (274)	1.65 (0.11)	7.1
11	Shrubs and bare ground	255 (147)	17.0 (8.2)	3106 (390)	3490 (524)	5.50 (0.42)	11.0
12	Cultivation	755 (443)	13.6 (8.2)	2508 (518)	3260 (850)	1.73 (0.06)	13.3

lies and positively correlated with temperature anomalies in the boreal forest biome (biome 4 in table 1, and Figure 2(d) and (e)). For those biomes dominated by shrubs and bare ground, wooded C4 grassland, and C4 grassland, significant correlations exist between the CGR and biome temperature anomalies (Figure 2(f)—(h)). The correlation was significantly improved by including data for the year of 1987 for the wooded C4 grassland and C4 grassland biomes. The C3 wooded grassland biome is more sensitive to the perturbations of PAR and drought stress than the other climatic variables examined.

Except for the biomes shown in Figure 2, the biome of broadleaf deciduous forest and woodland has a weak positive correlation between CGR and temperature (r=0.43), but it is not statistically significant (p=0.11). Although the other biomes, i.e., high latitude deciduous forest and woodland, tundra and C3 grassland, cover relatively large area (24.4% of total land area), there does not exist apparent correlation between them.

The high correlation between the CGR and precipitation anomalies (Figure 2(a) and (b)) implies that a dryer year will cause an increase in tropical rain forest CO_2 uptake. This implication is in contrast with the traditional concept used by modellers in which water availability limits tree growth, potentially reducing CO_2 uptake in dryer years[31,32]. We hypothesize that photosynthesis is less sensitive to water stresses than heterotrophic respiration for tropical rain forest ecosystems. The physical reason behind this hypothesis is that trees in the tropical rain forest are able to tap deep water for the maintenance of photosynthesis in dryer years[33], but the decomposition of soil organic matter concentrated near the surface is inhibited. This hypothesis is supported by eddy flux tower measurements and biometric observations conducted in two old-growth tropical forest sites near Santarem, Brazil[34]. Three years' eddy flux data showed that carbon was taken up in the dry season and released in the wet season; this opposes the predictions of two ecosystem models[31,32], but is consistent with the trends presented in Figure 2.

The CGR is positively correlated to precipitation anomalies and negatively to dryness anomalies for the C3 wooded grassland (Figure 2(j) and (k)). This could be attributed to different sensitivity of net primary production (NPP) and soil respiration on precipitation change. To identify the impact of precipitation anomaly on NPP and soil respiration, the soil respiration model[35] and CASA-NPP model[36,37] were applied to conducting the sensitivity analysis. The results show that soil respiration in C3 wooded grassland will increase by 1.3% and NPP will increase by 2.4%, respectively, if precipitation alone increased by 20%. On condition that the negative correlation between PAR and precipitation (Figure 3) was considered, the modelled NPP caused by both precipitation and PAR only increases by 0.45%, which is much less than soil respiration, i.e., 1.3%.

Generally, higher CO_2 growth rates correspond to El Niño climate conditions[38,39]. There exist direct and indirect impacts of El Niño on CGR. The direct impact is

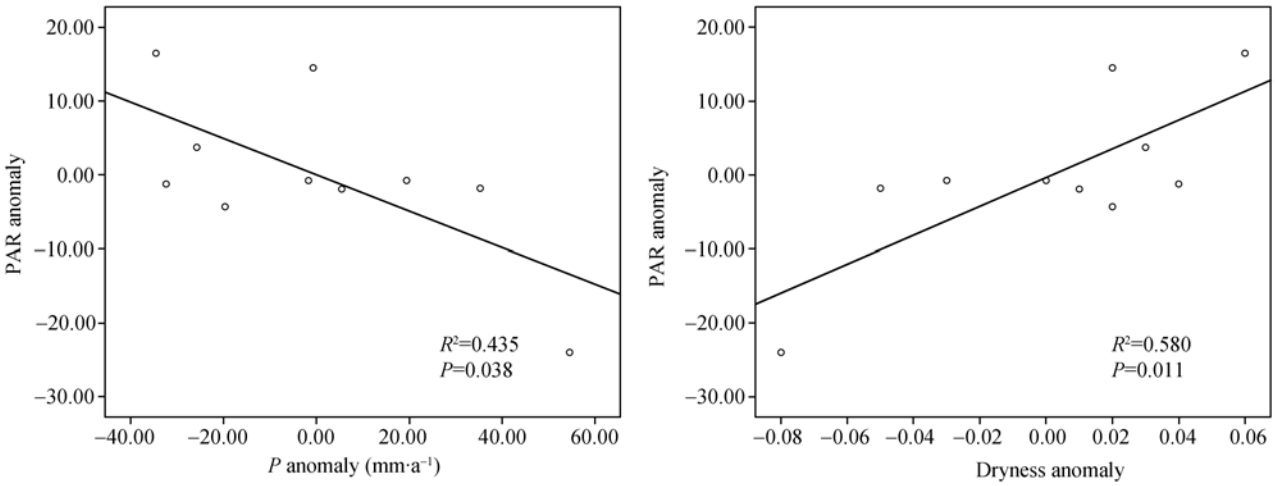

Figure 3 Relationship between PAR anomaly and precipitation (*P*) and dryness anomaly for C3 wooded grassland.

that El Niño changes the temperature and precipitation, which controls the magnitude of land-atmosphere fluxes and associates with the year-to-year fluctuations of CGR[17,40]. The indirect one is that co-varying processes such as reduced productivity caused by drought in tropical forests during El Niño episodes may be superimposed on fire emissions, which appear to contribute to high CO_2 growth during the El Niño episodes[41−45].

One previous study has shown that a highly positive correlation exists between atmospheric CO_2 anomaly and anomalous sea surface temperature (SST) in the equatorial Pacific during an El Niño year[46]. This might suggest that our observation in 1987, a strong El Niño year, as an outlier in the data set of Figure 2, is due to an episodic ocean influence on the CGR, rather than terrestrial biome influences. However, the explanation that increased SST leads to the above average release of CO_2 from the equatorial Pacific was questioned by Hyson and Pearman[47] who argued that the effect of temperature on the partial pressure of CO_2 in the water was not sufficient to account for the observed atmospheric signal. Furthermore, sea-surface CO_2 partial pressure measurements from the equatorial Pacific have shown reduction, other than increase, in CO_2 emissions during this El Niño event due to the reduced upwelling of CO_2-eriched water[48]. Thus, the potential remains for terrestrial ecosystems to influence the CGR during years of anomalous climate, although the results in Figure 2(a) and (b) suggest that it is not the influence of precipitation, and coupled dryness, and anomalies that exert the principal influence during the 1987 El Niño.

It is worthwhile to note that 1987 was not peculiar in the relation between the CGR and temperature anomaly in tropical forests (Figure 2(c)) in contrast with the results presented for precipitation and dryness (Figure 2(a) and (b)). The correlation that includes 1987 is better than the correlation without 1987, suggesting that the atmospheric CO_2 anomaly observed for 1987 may be the result of temperature driving more CO_2 release to the atmosphere from the tropical rainforest.

The CGR was negatively correlated with PAR anomalies and positively correlated with temperature anomalies in the boreal forest biome (biome 4 in table 1, and Figure 2(d) and (e)). These two parameters are not necessarily independent of each other; the degree of cloudiness of any given day is likely to influence its temperature. The intuitive connections of these anomalies to photosynthesis and respiration appear to be in the direction consistent with their effects on the CGR; anomalies with higher PAR should cause higher rates of photosynthesis, and thus should cause a decrease in CGR as observed; anomalies with higher temperature should cause higher respiration rates[49], and thus should cause an increase in the CGR, as observed.

Overall, our analysis suggests that the tropical rainforest, wooded C4 grassland, and C4 grassland were the sources for the 1987 atmospheric CO_2 anomaly driven by temperature. These three biomes occupy 30% of the total global land surface area and have an important effect on global atmospheric CO_2 growth rate. Since the Third Assessment Report of the Intergovernmental Panel on Climate Change, many studies have confirmed that the variability of CO_2 fluxes is mostly due to land fluxes, and that tropical lands contribute strongly to this sig-

nal[7]. For instance, three different inversion ensembles from Bousquet et al.[14], Rödenbeck et al.[15] and Baker et al.[16] also indicate that tropical rainforest and nearby grassland make the greatest contribution to the interannual variation of land-atmosphere fluxes in the year of 1987. Although the correlation between the CGR and temperature anomaly of biomes with shrubs and bare ground is significant, we would not attribute these biomes to a major source for the 1987 anomaly because their potential for atmospheric carbon assimilation and storage is low.

Our results have two important and clear implications. First, our results indicate that the largest atmospheric CO_2 anomaly, during the El Niño year of 1987, was caused by tropical biomes (tropical rainforest, wooded C4 grassland, and C4 grassland) as they responded to temperature. Second, the tropical rain forest, boreal forest, tropical savanna and C4 grassland are the major climate-sensitive sources/sinks for the interannual variability of atmospheric CO_2. These four biomes occupy 39% of the total global land surface area (Table 1) and account for approximately 57% of the total land carbon storage[1]. Each of these biomes, however, influences the CGR through unique responses to climate perturbations. Our correlation analysis indicates that the boreal forest influences the CGR through responses to anomalies in PAR and temperature; the tropical rainforest influences the CGR through responses to anomalies in drought; all of the tropical biomes influence the CGR through responses to anomalies involving temperature.

3 Conclusions

Biome scale analysis shows that the interannual variation in atmospheric CO_2 concentration is coupled to the responses of four major global biomes (tropical rainforest, tropical savanna, C_4 grassland and boreal forest) and their photosynthetic and respiratory responses to different climate factors. Our results are especially powerful in explaining the influence of one of the strongest El Niño climate anomalies in the past two decades on the atmospheric CO_2 concentration; this relationship appears to be predominantly driven by responses of the tropical biomes to El Niño climate conditions. Overall, our work shows that the most climate-sensitive sources/sinks of atmospheric CO_2 originate from tropical biomes, a finding being in contrast to previous studies that have concluded that the largest component of the missing carbon sink resides in the Northern Hemisphere.

The authors thank two anonymous reviewers for their constructive suggestions. The authors are grateful to Prof. Russ Monson (CU Boulder) for valuable discussion. The authors also thank Dr. Paul W. Stackhouse (NASA) for providing the monthly global datasets of surface shortwave (SW) and long wave (LW) fluxes with 1°×1° resolution.

1 Houghton J T, Ding Y, Griggs D J, et al. Climate Change 2001: The Scientific Base. Cambridge: Cambridge University Press, 2001. 1－896
2 Schimel D S, House J I, Hibbard K A, et al. Recent patterns and mechanisms of carbon exchange by terrestrial ecosystems. Nature, 2001, 414: 169－172[DOI]
3 Wofsy S C. Where has all the carbon gone? Science, 2001, 292: 2261－2263 [DOI]
4 Tans P P, Fung I Y, Takahashi T. Observational constraints on the global atmospheric CO_2 budget. Science, 1990, 247: 1431－1438[DOI]
5 Conway T J, Tans P P, Waterman L S, et al. Evidence for interannual variability of the carbon cycle from the National Oceanic and Atmospheric Administration/Climate Monitoring and Diagnostics Laboratory Global Air Sampling Network. J Geophys Res, 1994, 99: 22831－22855[DOI]
6 Keeling C D, Whorf T P, Wahlen M, et al. Interannual extremes in the rate of rise of atmospheric carbon dioxide since 1980. Nature, 1995, 375: 666－670[DOI]
7 Denman K L, Brasseur G, Chidthaisong A, et al. Couplings between changes in the climate system and biogeochemistry. In: Solomon S, Qin D, Manning M, et al, eds. Climate Change 2007: The Physical Science Basis. New York: Cambridge University Press, 2007. 499－587
8 Gurney K R, Law R M, Denning A S, et al. Towards robust regional estimates of CO_2 sources and sinks using atmospheric transport models. Nature, 2003, 415: 626－630[DOI]
9 Rayner P J, Enting I G, Francey R J, et al. Reconstructing the recent carbon cycle from atmospheric CO_2, $\delta^{13}C$ and O_2/N_2 observations. Tellus Ser B-Chem Phys Meteorol, 1999, 51: 213－232
10 Houghton R A. Revised estimates of the annual net flux of carbon to the atmosphere from the changes in land use and land management 1850－2000. Tellus Ser B-Chem Phys Meteorol, 2003, 55: 378－390
11 Lee K, Wanninkhof R, Takahashi T, et al. Low interannual variability in recent oceanic uptake of atmospheric carbon dioxide. Nature, 1998, 396: 155－159[DOI]
12 Quéré C L, Aumont O, Bousquet P, et al. Two decades of ocean CO_2 sink and variability. Tellus Ser B-Chem Phys Meteorol, 2003, 55: 649－656
13 McKinley G A, Follows M J, Marshall J. Mechanisms of air-sea CO_2 flux variability in the equatorial Pacific and the North Atlantic. Globl Biogeochemcl Cycles, 2004, 18: GB2011, doi: 10.1029/2003GB002179
14 Bousquet P, Peylin P, Ciais P, et al. Regional changes in carbon dioxide fluxes of land and oceans since 1980. Science, 2000, 290:

1342－1346[DOI]
15 Rödenbeck C, Houweling S, Gloor M, et al. Timedependent atmospheric CO_2 inversions based on interannually varying tracer transport. Tellus Ser B-Chem Phys Meteorol, 2003, 55: 488－497
16 Baker D F, Law R M, Gurney K R, et al. TransCom 3 inversion intercomparison: Impact of transport model errors on the interannual variability of regional O_2 fluxes, 1988－2003. Glob Biogeochem Cycle, 2006, 20: GB1002, doi: 10.1029/2004GB002439
17 Jones C D, Cox P M. Constraints on the temperature sensitivity of global soil respiration from the observed interannual variability in atmospheric CO_2. Atmos Sci Lett, 2001, 1, doi: 10.1006/asle.2001.0041
18 McGuire A D, Sitch S, Clein J S, et al. Carbon balance of the terrestrial biosphere in the twentieth century: Analyses of CO_2, climate and land use effects with four process-based ecosystem models. Globl Biogeochem Cycle, 2001, 15: 183－206[DOI]
19 Peylin P, Bousquet P, Quéré C, et al. Multiple constraints on regional CO_2 flux variations over land and oceans. Glob Biogeochem Cycle, 2005, 19: GB1011, doi: 10.1029/2003GB002214
20 Zeng N, Mariotti A, Wetzel P. Terrestrial mechanisms of interannual CO_2 variability. Globl Biogeochem Cycle, 2005, 19: GB1016, doi:10.1029/2004GB002273
21 Global View-CO_2: Cooperative Atmospheric Data Integration Project —— Carbon Dioxide. Boulder: NOAA/CMDL, 2003
22 DeFries R S, Townshend J R G. NDVI-derived land cover classifications on a global scale. Int J Remote Sens, 1994, 15: 3567－3586[DOI]
23 Matthews E. Global vegetation and land use: New high resolution data bases for climate studies. J Clim Appl Meteorol, 1983, 22: 474－487[DOI]
24 Olson J S, Watts J, Allison L. Carbon in Live Vegetation of Major World ecosystems. Oak Ridge National Laboratory Report ORNL-5862. 1983
25 Wilson M F, Sellers A. A global archive of land cover and soils data for use in general circulation models. J Climatol, 1985, 5: 119－143 [DOI]
26 Legates D R, Willmott C J. Mean seasonal and spatial variability in global surface air temperature. Theor Appl Climatol, 1990, 41: 11－21[DOI]
27 Rudolf B. Management and analysis of precipitation data on a routine basis. In: Proceedings of Int WMO/IAHS/ETH Symposium on Precipitation and Evaporation. Bratislava: Slovak Hydrometeor Institute, 1993. 69－76
28 Pinker R T, Laszlo I. Modeling surface solar irradiance for satellite applications on global scale. J Appl Meteor, 1992, 31: 194－211[DOI]
29 Clark D A, Piper S C, Keeling C D, et al. Tropical rain forest tree growth and atmospheric carbon dynamics linked to interannual temperature variation during 1984-2000. Proc Nat Acad Sci U S A, 2003, 100: 5852－5857[DOI]
30 Sotta E D, Meir P, Malhi Y, et al. Soil CO_2 efflux in a tropical forest in the central Amazon. Glob Change Biol, 2004, 10: 601－617[DOI]
31 Tian H, Melillo J M, Kicklighter D W, et al. Effect of interannual climate variability on carbon storage in Amazonian ecosystems. Nature, 1998, 396: 664－667[DOI]
32 Botta A, Ramankutty N, Foley J A. Long-term variations of climate and carbon fluxes over the Amazon basin. Geophys Res Lett, 2002, 29(9): 1319, doi:10.1029/2001GL013607
33 Nepstad D C, Carvalho C D, Davidson E A, et al. The role of deep roots in the hydrological and carbon cycles of Amazonian forests. Nature, 1994, 372: 666－669[DOI]
34 Saleska S R, Miller S D, Matross D M, et al. Carbon in Amazon forests: Unexpected seasonal fluxes and disturbance-induced losses. Science, 2003, 302: 1554－1557[DOI]
35 Raich J W, Potter C S, Bhagawati D. Interannual variability in global soil respiration, 1980－94. Glob Change Biol, 2002, 8: 800－812[DOI]
36 Potter C S, Randerson J T, Field C B, et al. Terrestrial ecosystem production: A process model based on global satellite and surface data. Glob Biogeochem Cycle, 1993, 7(4): 811－841
37 Field CB, Randerson J T, Malmstrom C M. Global net primary production: Combining ecology and remote sensing. Remote Sens Environ, 1995, 51:74－88[DOI]
38 Bacastow R B, Keeling C D. Atmospheric carbon dioxide concentration and the observed airborne fraction. In: Bolin B, ed. Carbon Cycle Modelling (SCOPE 16). New York: John Wiley and Sons, 1981. 103－112
39 Lintner B R. Characterizing global CO_2 interannual variability with empirical orthogonal function/principal component (EOF/PC) analysis. Geophys Res Lett, 2002, 29(19): 1921, doi: 10.1029/2001GL014419
40 Gérard J C, Nemry, B, Francois L M, et al. The interannual change of atmospheric CO_2: Contribution of subtropical ecosystems. Geophys Res Lett, 1999, 26: 243－246[DOI]
41 Barbosa P M, Stroppiana D, Grégoire J M, et al. An assessment of vegetation fire in Africa (1981－1991): Burned areas, burned biomass, and atmospheric emissions. Glob Biogeochem Cycle, 1999, 13(4): 933－950[DOI]
42 Langenfelds R L, Francey, R J, Pak B C, et al. Interannual growth rate variations of atmospheric CO_2 and its ^{13}C, H_2, CH_4, and CO between 1992 and 1999 linked to biomass burning. Glob Biogeochem Cycle, 2002, 16(3): 1048, doi: 10.1029/2001GB001466
43 Page S, Siegert F, Rieley J O, et al. The amount of carbon released from peat and forest fires in Indonesia during 1997. Nature, 2002, 320: 61－65[DOI]
44 Werf G R, Randerson J T, Collatz G J, et al. Carbon emissions from fires in tropical and subtropical ecosystems. Glob Change Biol, 2003, 9: 547－562[DOI]
45 Patra P K, Ishizawa M, Maksyutov S, et al. Role of biomass burning and climate anomalies for land-atmosphere carbon fluxes based on inverse modeling of atmospheric CO_2. Glob Biogeochem Cycle, 2005, 19: GB3005, doi: 10.1029/2004GB002258
46 Elliott W P, Angell J K. On the relation between atmospheric CO_2 and equatorial sea-surface temperature. Tellus Ser B-Chem Phys Meteorol, 1987, 39: 171－183
47 Hyson P, Pearman G I. Aspects of atmospheric CO_2 observations and modelling. In: Pearman G I, ed. Carbon Dioxide and Climate: Australian Research. Canberra: Australian Academy of Science, 1980. 65－77
48 Wong C S, Chan Y H, Page J S, et al. Change in equatorial CO_2 flux and new production estimated from CO_2 and nutrient levels in Pacific surface waters during the 1986/87 El Niño. Tellus Ser B-Chem Phys Meteorol, 1993, 45: 64－79 [DOI]
49 Goulden M L, Wofsy S C, Harden J W, et al. Sensitivity of Boreal Forest Carbon Balance to Soil Thaw. Science, 1998, 279: 214－217[DOI]